JOURNAL OF MATERIALS SCIENCE **40** (2005) 927–932

Weld decay-resistant austenitic stainless steel by grain boundary engineering

H. KOKAWA
Department of Materials Processing, Graduate School of Engineering, Tohoku University, Aoba-Yama 02, Sendai 980-8579, Japan
E-mail: kokawa@material.tohoku.ac.jp

This paper presents an example of grain boundary engineering (GBE) for improving intergranular-corrosion and weld-decay resistance of austenitic stainless steel. Transmission and scanning electron microscope (TEM and SEM) observations demonstrated that coincidence site lattice (CSL) boundaries possess strong resistance to intergranular precipitation and corrosion in weld decay region of a type 304 austenitic stainless steel weldment. A thermomechanical treatment for GBE was tried for improvement of intergranular corrosion resistance of the 304 austenitic stainless steel. The grain boundary character distribution (GBCD) was examined by orientation imaging microscopy (OIM). The sensitivity to intergranular corrosion was reduced by the thermomechanical treatment and indicated a minimum at a small roll-reduction. The frequency of CSL boundaries indicated a maximum at the small roll-reduction. The corrosion rate was much smaller in the thermomechanical-treated specimen than in the base material for long time sensitization. The optimum thermomechanical treatment introduced a high frequency of CSL boundaries and the clear discontinuity of corrosive random boundary network in the material, and resulted in the high intergranular corrosion resistance arresting the propagation of intergranular corrosion from the surface. The optimized 304 stainless steel showed an excellent resistance to weld decay during arc welding.

1. Introduction

One of the biggest problems during welding of austenitic stainless steel is intergranular corrosion in the heat-affected zone (HAZ), so called "weld decay" [1, 2]. The intergranular corrosion is attributed to sensitization. Sensitization by chromium depletion due to chromium carbide precipitation at grain boundaries in austenitic stainless steels can not be prevented perfectly only by previous conventional techniques, such as reduction of carbon content, stabilization-treatment, local solution-heat-treatment, etc. Recent studies on grain boundary structure have revealed that the sensitization depends strongly on crystallographic nature and atomic structure of the grain boundary, and that low energy grain boundaries such as CSL boundaries have strong resistance to intergranular corrosion [3]. The concept of 'grain boundary design and control' [4] has been developed as GBE [5]. GBEed materials which are characterized by high frequencies of CSL boundaries are resistant to intergranular deterioration of materials, such as intergranular corrosion [6–8].

We have been trying to produce a GBEed austenitic stainless steel possessing a strong resistance to weld decay using an identical 304 steel [9–14]. This paper shows the progress reviewing our previous work [9–14] with some new data. TEM observations in the weld HAZ [9] and the isothermal heat-treated specimens [10, 11] have proved that low-Σ CSL boundaries require longer time for intergranular chromium carbide precipitation and corrosion than random boundaries. An optimized thermomechanical treatment for the 304 steel resulted in excellent intergranular corrosion resistance due to optimized grain boundary character distribution (GBCD), i.e., the uniform distribution of a high frequency of CSL boundaries and consequent discontinuity of random boundary network in the material [12]. The GBEed 304 steel was gas-tungsten-arc (GTA) welded and the resistance to weld decay for the GBEed 304 steel was examined by corrosion tests and OIM [15].

2. Experimental procedures

A commercial type 304 austenitic stainless steel was used throughout this study. The chemical composition (wt%) is 18.28 Cr, 8.48 Ni, 0.60 Si, 1.00 Mn, 0.055 C, 0.029 P and 0.005 S. The base material plate of $9 \times 50 \times 150$ mm^3 was welded by bead-on-plate GTA welding at a welding current of 300A in direct current electrode negative (DCEN), a travel speed of 4 cm/min, an arc length of 1 mm without filler materials in a welding chamber filled with argon gas.

For thermomechanical treatment as GBE, the initial size of the base material specimen was $9 \times$

10×35 mm^3. The specimens were solution-heat-treated at 1323 K for 0.5 h. Thermomechanical treatment was performed by cold-rolling and subsequent annealing. The roll reduction ratio in thickness as pre-strain was varied from 0 to 60%. The pre-strained specimens were annealed at various temperatures from 1200 to 1600 K and quenched in cold water. The GBCD was examined by OIM. In this study, grain boundaries with $\Sigma \leq 29$ were regarded as low-Σ CSL boundaries since special properties have been reported in CSL boundaries with $\Sigma \leq 29$ [10, 16], and Brandon's criterion [17] was adopted for the critical deviation in the grain boundary characterization [10, 18]. The intergranular corrosion resistance was evaluated by a double loop electrochemical potentiokinetic reactivation (DL-EPR) test [19] after sensitization treatment at 923 K. The base material (BM) and 5% strain-annealed (r5%) specimens were assessed by a ferric sulfate-sulfuric acid test [20] after sensitization at 923 K. The tested specimens were observed by SEM.

The as-received and the GBDed (thermomechanically treated) materials of the 304 steel were GTA-welded and the weld HAZs were observed by SEM and TEM, and examined by corrosion test and OIM.

3. Results and discussion

3.1. Grain boundary character and intergranular precipitation in weld decay

The weld decay region is located in the HAZ of the welded specimen of the as-received 304 steel plate as schematically illustrated in the upper part of Fig. 1. The optical micrograph of the weld decay region in the lower part of Fig. 1 shows a mixed structure of grooved and non-grooved boundaries by 10% oxalic acid electro-etching. The difference in grooving can depend on grain boundary energy [10]. Fig. 2 shows grain boundaries in the weld decay region after 10% oxalic acid electro-etching. Figs 2a and b are micrographs taken from an area by optical microscope and SEM, respectively. Electron channeling patterns (ECPs) obtained from grains A, B and C are also indicated in Fig. 2. The grain boundary GB1 has no groove, while GB2 and GB3 are deeply grooved. GB1 is regarded as a Σ5-boundary, because the misorientation is deviated only 2.55 degrees from exact Σ5 CSL, i.e. $\Delta\theta/\Delta\theta c = 0.38$, where $\Delta\theta c$ is the critical deviation angle derived by Brandon's criterion for the Σ CSL misorientation. GB2 and GB3 are random boundaries, because their $\Delta\theta/\Delta\theta c$ are 1.76 and 2.27, respectively. The relationship between misorientation and grooving for 40 grain boundaries in the weld decay region was examined. The 27 grooved boundaries were random boundaries, while all of the low-Σ CSL boundaries ($\Sigma \leq 29$) were not grooved. Since the 10% oxalic acid etching is sensitive to precipitation, low energy grain boundaries with low-Σ CSL misorientations have stronger resistance to intergranular precipitation than high energy random boundaries in the weld decay region. TEM observations in the weld decay region have revealed that some grain boundaries accept precipitation, but some do not. For example, no precipitation is seen at the grain boundary in Fig. 3a, while Cr-rich $M_{23}C_6$ precipitates are observed at the grain boundary in Fig. 3b. Their misorientations correspond to a Σ9 boundary in Fig. 3a and a random boundary in Fig. 3b. The relationship between misorientation and precipitation for 125 grain boundaries in the weld decay region was examined. The 67 grain boundaries with precipitation were random boundaries, while all of the low-Σ CSL boundaries ($\Sigma \leq 29$) were free from precipitation. Trillo and Murr [21, 22] have reported a remarkable resistance of coherent twin boundary to carbide precipitation because of extreme low boundary energy. Low energy CSL boundaries hardly accept intergranular precipitation compared with high energy random boundaries in the weld decay region.

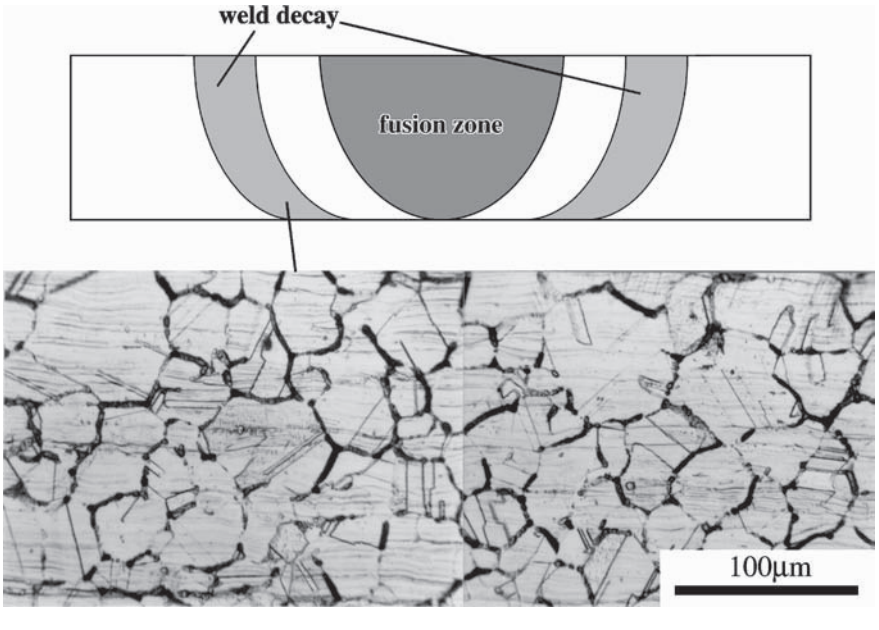

Figure 1 A mixed structure of grooved and non-grooved boundaries in the weld decay region of the weld-HAZ of the initial 304 austenitic stainless steel after 10% oxalic acid electro-etching [10].

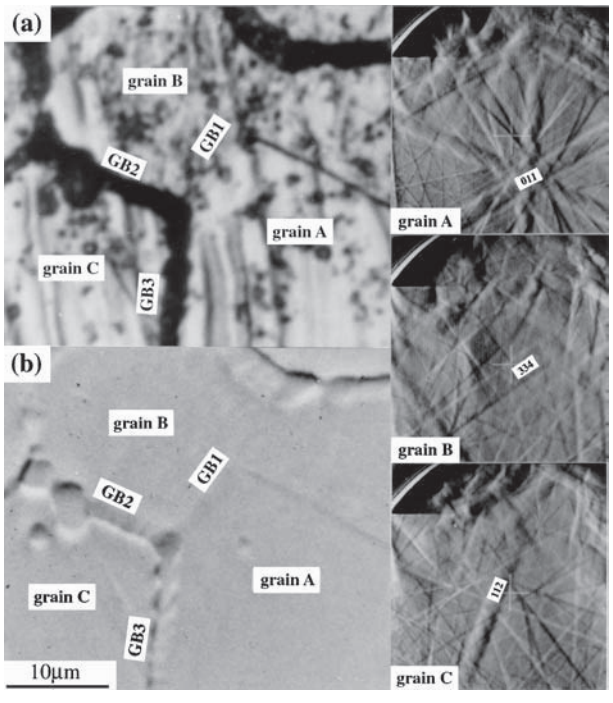

Figure 2 (a) Optical and (b) SEM micrographs of grain boundaries in the weld decay region of the initial 304 austenitic stainless steel after 10% oxalic acid electro-etching, and ECPs obtained from grains A, B and C in (a) and (b) [9].

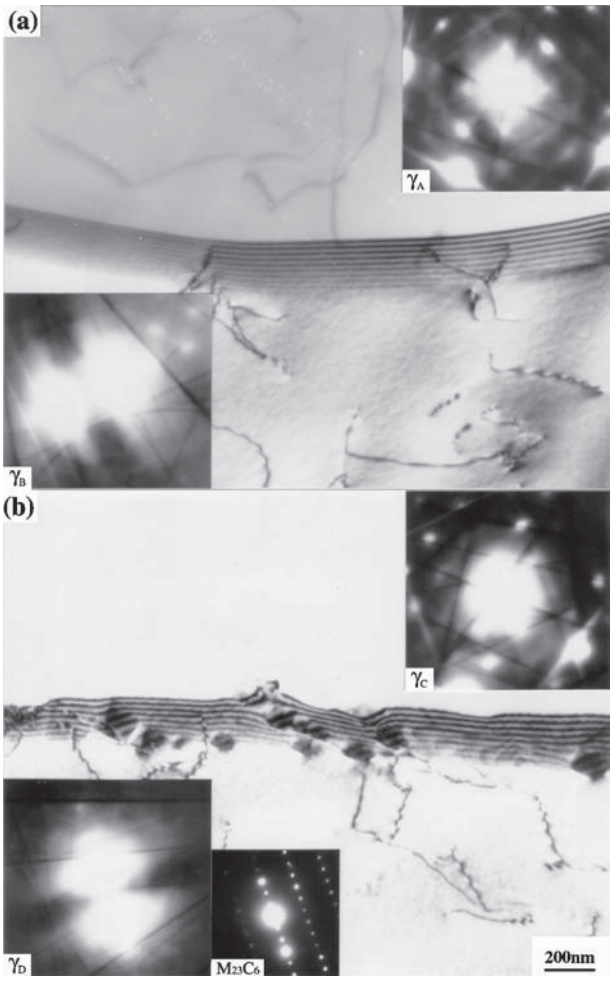

Figure 3 TEM micrographs of (a) Σ9 and (b) random grain boundaries in the weld decay region of the initial 304 austenitic stainless steel [10].

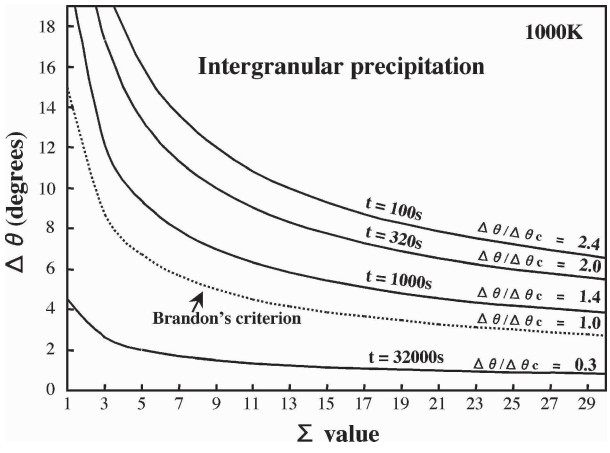

Figure 4 Intergranular carbide precipitation and the deviation angle from the CSL misorientation in the initial 304 austenitic stainless steel during sensitization at 1000 K [10].

TEM observations were carried out for the as-received 304 steel after sensitization at 1000 K for 100–32000 s. The relationship between intergranular carbide precipitation and grain boundary misorientation was examined. Fig. 4 shows the borderlines between grain boundary precipitation and no precipitation during sensitization at 1000 K for different times of period [10]. In the figure, the Σ-value of the nearest CSL ($\Sigma \leq 29$) was taken as the abscissa, and the deviation angle $\Delta\theta$ from the exact CSL misorientation was taken as the vertical axis. Increases in $\Delta\theta$ and Σ-value mean decrease in the regularity of grain boundary structure [3] and roughly mean increase in the grain boundary energy [23]. The grain boundaries with lower regularities and with higher energies in the region above the borderline accept intergranular precipitation at the sensitization time. The borderlines can be described by $\Delta\theta/\Delta\theta$c, i.e. $\Delta\theta/\Delta\theta c = 2.4$, 2.0, 1.4 and 0.3 for 100, 320, 1000 and 32000 s, respectively. The figure reveals that a more ordered boundary needs longer time for carbide precipitation and corrosion than a less ordered boundary. This tendency may result from more difficult nucleation and a lower growth rate of carbide at a more ordered boundary because of lower grain boundary energy. The $\Delta\theta/\Delta\theta$c decreases with an increase of sensitization time at 1000 K. If the grain boundary structure could be kept with a smaller $\Delta\theta/\Delta\theta$c than the borderline for each sensitization time by GBE, intergranular precipitation and corrosion would not occur. Since the $\Delta\theta/\Delta\theta$c is much larger than 1 at a short sensitization time, the character as a Σ-boundary may be valid with somewhat larger deviations than Brandon's criterion for a shorter time sensitization. This suggests that the conditions to prevent intergranular carbide precipitation by controlling grain boundary character are not very severe for a short time exposure to a sensitizing temperature, such as in welding thermal cycles. GBE can inhibit the weld decay of austenitic materials.

3.2. Grain boundary engineering for suppression of weld decay

The feasibility of GBE has been demonstrated mainly by thermomechanical treatments, which can be broadly

divided into strain recrystallization and strain annealing processes [6, 7, 24–30]. Palumbo *et al*. have improved the intergranular corrosion susceptibility in nickel base alloys by the strain recrystallization process [5–7, 30]. King *et al*. have reported evolution of the GBCD in Cu by the strain annealing process [25, 27]. Kumar *et al*. found that the network of random boundaries in Inconel 600 was broken-up by twin formation during the sequential thermomechanical treatment [29]. Generation of $\Sigma 3^n$ CSL boundaries by twin events [8] during thermomechanical treatment can increase the frequency of CSL boundaries in the fcc based materials, but may not always result in the optimum GBCD. Recently, the present authors [12] have demonstrated that a slight pre-strain annealing at a relatively low temperature results in excellent intergranular corrosion resistance due to optimized GBCD in type 304 austenitic stainless steel. The effects of the roll reduction ratio as pre-strain on the reactivation current ratio during the DL-EPR test after sensitization treatment and on the frequency of CSL boundaries in the thermomechanically treated 304 steel indicated an optimum pre-strain of 5% in strain annealing at 1300 K in the GBE process of this material. The effect of annealing temperature at 5% pre-strain on the GBCD was examined by OIM. The annealing temperature and time were varied to find the process parameters needed to achieve the optimum GBCD. Annealing at 1400 K and higher temperatures did not result in any better differences in the GBCD compared with that at 1300 K, but a favorable change in the GBCD was observed during annealing at 1200 K, i.e., with increasing annealing time at 1200 K, a high CSL frequency layer (about 85% CSL) was formed near the rolled surface and expanded into the specimen. Fig. 5 shows the developing front of the high CSL frequency layer at about 2 mm from the surface of the specimen annealed at 1200 K for 48 h. The OIM indicates that the high CSL frequency area including random boundary debris remained in the right side whereas the continuous random boundary network remained in the left side. A uniform distribution of the high CSL frequency area was achieved in the r5% specimen annealed at 1200 K for 72 h (r5%-1200 K-72 h). The frequency of CSL boundaries was homogeneous to be 86.5% in the specimen with a thickness of about 10 mm. Some of the areas surrounded by random boundaries are larger than 0.5 mm in diameter. A number of twins formed in the growing grains compensate grain-coarsening. The network of random grain boundaries in the as-received base material was totally disrupted, and short random boundary segments were isolated in the r5%-1200 K-72 h specimen. The differences in GBCD between the BM, r5%-1300 K-0.5 h, r5%-1200 K-48 h and the r5%-1200 K-72 h specimens are schematically illustrated in Fig. 6.

The DL-EPR test results reflect the fractional area of chromium depletion near sensitized grain boundaries on the test surface. The actual intergranular corrosion propagates along grain boundaries from the surface into the material and causes mass-loss due to grain dropping. The corrosion (mass loss) rate during the ferric sulfate-sulfuric acid test is shown in Fig. 7 for the BM,

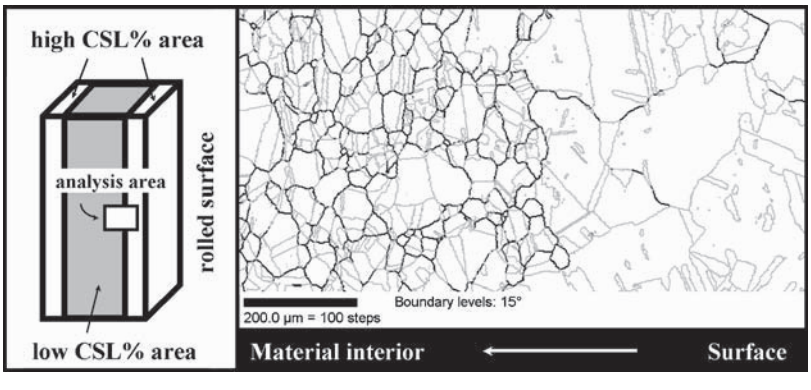

Figure 5 GBCD by OIM in the border area at the front of the high CSL frequency layer in the r5%-1200 K-48 h thermomechanically treated specimen [12].

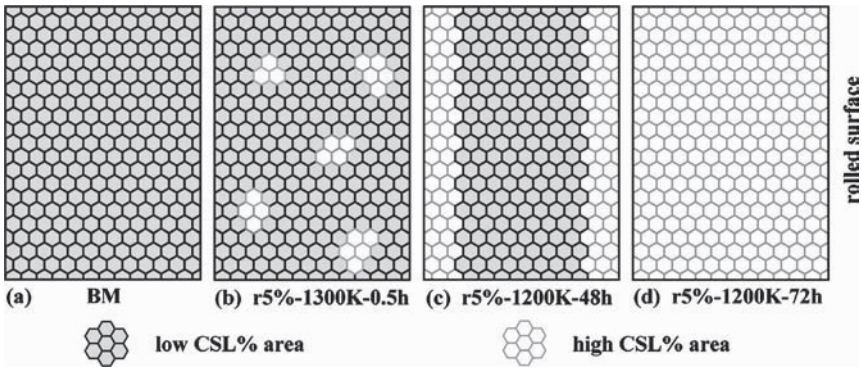

Figure 6 Schematic illustration of the GBCD in the initial material (BM) (a), and thermomechanically treated specimens with different parameters (b), (c) and (d) [12].

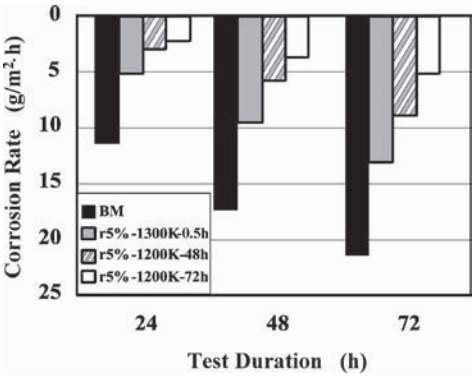

Figure 7 The corrosion mass-loss of the BM and the strain-annealed specimens during the ferric sulfate-sulfuric acid test [12].

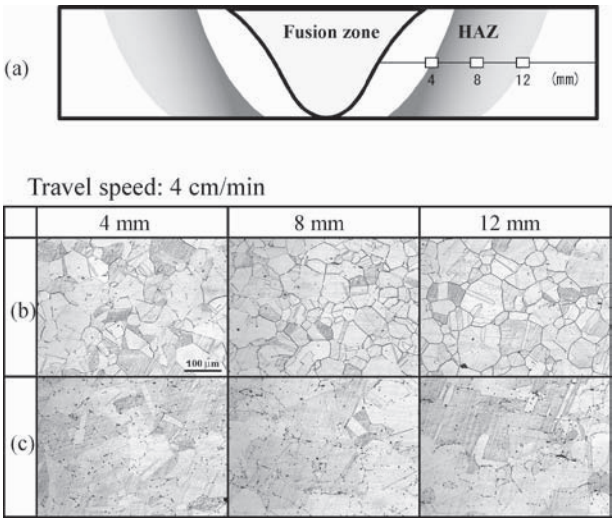

Figure 8 Optical micrographs of the areas at 4, 8 and 12 mm away from the fusion line in the weld HAZ for the as-received base material (b) and the GBEed specimen (c), respectively, indicated the locations schematically in (a).

r5%-1300 K and r5%-1200 K specimens after sensitization. The strain-annealed specimens have much lower corrosion rates than the BM for every test duration. The difference in mass-loss is much more than that expected simply from differences in DL-EPR test results and CSL boundary frequencies, because the improvement in GBCD can strongly affect the mass-loss. The r5%-1200 K-72 h specimen with the optimized GBCD (Fig. 6d) indicated the smallest corrosion rate, which was less than one-fourth that of the BM, and less than half that of the r5%-1300 K-0.5 h specimen. The corrosion rate of the r5%-1200 K-48 h specimen with high CSL frequency layers (Fig. 6c) was higher than that of the r5%-1200 K-72 h specimen with a uniformly high CSL frequency (Fig. 6d), but smaller than that of the r5%-1300 K-0.5 h specimen with randomly distributed high CSL frequency areas (Fig. 6b) [12].

The optimum distribution can be achieved by introduction of low-energy segments on migrating random boundaries during twin emission and boundary-boundary reactions in the grain growth without generation of new random boundaries [12]. Well-distributed low-energy segments in the grain boundary network create a discontinuous chain of chromium depletion and can arrest the percolation of intergranular corrosion from the surface [12]. An analytical transmission electron microscopic study of thermomechanically treated 304 austenitic stainless steel demonstrated that the chromium depletion at a low-energy boundary segment introduced by twin-emission into a random boundary was smaller than that of the original random boundary after sensitization [14].

In order to examine the effect of GBE on the weld decay in 304 austenitic stainless steel, the r5%-1200 K-72 h specimen with the optimized GBCD and the as-received 304 base material were GTA-welded. The HAZ of each weld was observed after electro-etched in an oxalic acid solution. Fig. 8a shows the schematic illustration of the observed areas at 4, 8 and 12 mm away from the fusion line in the HAZ on the mid thickness horizontal line. The optical micrographs of the areas are shown in Fig. 8b and c for the as-received base material and the GBEed specimen with the optimized GBCD, respectively. In the HAZ of the as-received base material, most of the grain boundaries are grooved in the areas at 8 and 12 mm as generally seen in weld decay. In contrast, almost none of grain boundaries are grooved through the HAZ of the GBEed material. Both the degree of sensitization by DL-EPR test and the corrosion rate during the ferric sulfate-sulfuric acid test were much lower in the weld of GBEed material than in that of the as-received 304 steel base material.

4. Conclusion

Grain boundary engineering was tried for improving intergranular-corrosion and weld-decay resistance of austenitic stainless steel. TEM and SEM observations of weld decay region in a type 304 stainless steel weldment demonstrated that CSL boundaries showed strong resistance to intergranular precipitation and corrosion. A thermomechanical treatment for GBE was tried for improvement in intergranular corrosion resistance of 304 austenitic stainless steel. The sensitivity to intergranular corrosion was reduced by the thermomechanical treatment and indicated a minimum at a small roll-reduction. The frequency of CSL boundaries indicated a maximum at the small roll-reduction. The corrosion rate in a ferric sulfate-sulfuric acid test was much smaller in the thermomechanical-treated specimen than in the base material for long time sensitization. The optimum thermomechanical treatment introduced a high frequency of CSL boundaries and the clear discontinuity of corrosive random boundary network in the material, and resulted in the high intergranular corrosion resistance arresting the propagation of intergranular corrosion from the surface. The optimized 304 stainless steel showed an excellent resistance to weld decay during arc welding.

Acknowledgments

The partial support of this study by a Grant-in-Aid for Specially Promoted Research (COE)(2) (No. 11CE2003) and a Grant-in-Aid for Scientific Research (B) (No.15360379) and for the 21st century

COE program in International Center of Research and Education for Materials at Tohoku University from the Japanese Ministry of Education, Culture, Sports, Science and Technology is gratefully acknowledged. The author wishes to thank Professor T. Watanabe, Professor Z. J. Wang, Dr. Y. S. Sato and Dr. M. Shimada for their useful advice, and Mr. A. Honda for his technical assistance.

References

1. E. FOLKHARD, "Welding Metallurgy of Stainless Steels" (Springer-Verlag, Vienna, 1988) p. 103.
2. S. KOU, "Welding Metallurgy" (John Wiley and Sons, New York, 1987) p. 369.
3. P. H. PUMPHREY, in "Grain Boundary Structure and Properties," edited. by G. A. Chadwick and D. A. Smith (Academic Press, London, 1976) p. 139.
4. T. WATANABE, *Res Mechanica* **11** (1984) 47.
5. G. PALUMBO, E. M. LEHOCKEY and P. LIN, *JOM* **50** (1998) 40.
6. E. M. LEHOCKEY, G. PALUMBO, P. LIN and A. M. BRENNENSTUHL, *Scripta Mater*. **36** (1997) 1211.
7. E. M. LEHOCKEY, G. PALUMBO and P. LIN, *Metall. Mater. Trans. A* **29A** (1998) 3069.
8. P. LIN, G. PALUMBO and K. T. AUST, *Scripta Mater.* **36** (1997) 1145.
9. H. KOKAWA and T. KUWANA, *Trans. Jpn. Weld. Soc.* **23** (1992) 73.
10. H. KOKAWA, M. SHIMADA and Y. S. SATO, *JOM* **52** (2000) 34.
11. H. KOKAWA, T. KOYANAGAWA, M. SHIMADA, Y. S. SATO and T. KUWANA, in "Properties of Complex Inorganic Solids 2," edited by A. Meike, A. Gonis, P. E. A. Turchi and K. Rajan (Kluwer Academic/Plenum Publishers, New York, 2000) p. 17.
12. M. SHIMADA, H. KOKAWA, Z. J. WANG, Y. S. SATO and I. KARIBE, *Acta Mater.* **50** (2002) 2331.
13. H. KOKAWA, M. SHIMADA, Z. J. WANG and Y. S. SATO, *Annales de Chimie, Science des Materaix* **27** (2002) S315.
14. H. Y. BI, H. KOKAWA, Z. J. WANG, M. SHIMADA and Y. S. SATO, *Scripta Mater.* **49** (2003) 219.
15. B. L. ADAMS, S. I. WRIGHT and K. KUNZE, *Metall. Trans. A* **24A** (1993) 819.
16. H. KOKAWA, T. WATANABE and S. KARASHIMA, *Philos. Mag. A* **44** (1981) 1239.
17. D. G. BRANDON, *Acta Metall.* **14** (1966) 1479.
18. H. KOKAWA, T. WATANABE and S. KARASHIMA, *Scripta Metall*. **21** (1987) 839.
19. A. P. MAJIDI and M. A. STREICHER, *Corrosion* **40** (1984) 584.
20. J. B. LEE, *ibid.* **39** (1983) 469.
21. E. A. TRILLO and L. E. MURR, *J. Mater. Sci.* **33** (1998) 1263.
22. *Idem.*, *Acta Mater.* **47** (1999) 235.
23. D. A. SMITH, *Scripta Metall.* **8** (1974) 1197.
24. C. B. THOMSON and V. J. RANDLE, *Mater. Sci.* **32** (1997) 1909.
25. W. E. KING and A. J. SCHWARTZ, *Scripta Mater.* **38** (1998) 449.
26. V. THAVEEPRUNGSRIPORN, P. SINSROK and D. THONG-ARAM, *ibid.* **44** (2001) 67.
27. A. J. SCHWARTZ and W. E. KING, *JOM* **50** (1998) 50.
28. V. RANDLE, *Acta Mater.* **47** (1999) 4187.
29. M. KUMAR, W. E. KING and A. J. SCHWARTZ, *ibid.* **48** (2000) 2081.
30. P. LIN, G. PALUMBO, U. ERB and K. T. AUST, *Scripta Metall. Mater.* **33** (1995) 1387.